JCI The Journal of Clinical Investigation

mTORC2 regulates renal tubule sodium uptake by promoting ENaC activity

Catherine E. Gleason, Gustavo Frindt, Chih-Jen Cheng, Michael Ng, Atif Kidwai, Priyanka Rashmi, Florian Lang, Michel Baum, Lawrence G. Palmer, David Pearce

J Clin Invest. 2015;125(1):117-128. https://doi.org/10.1172/JCI73935.

Research Article **Nephrology**

The epithelial Na^+ channel (ENaC) is essential for Na^+ homeostasis, and dysregulation of this channel underlies many forms of hypertension. Recent studies suggest that mTOR regulates phosphorylation and activation of serum/glucocorticoid regulated kinase 1 (SGK1), which is known to inhibit ENaC internalization and degradation; however, it is not clear whether mTOR contributes to the regulation of renal tubule ion transport. Here, we evaluated the effect of selective mTOR inhibitors on kidney tubule Na^+ and K^+ transport in WT and *Sgk1*$^{-/-}$ mice, as well as in isolated collecting tubules. We found that 2 structurally distinct competitive inhibitors (PP242 and AZD8055), both of which prevent all mTOR-dependent phosphorylation, including that of SGK1, caused substantial natriuresis, but not kaliuresis, in WT mice, which indicates that mTOR preferentially influences ENaC function. PP242 also substantially inhibited Na^+ currents in isolated perfused cortical collecting tubules. Accordingly, patch clamp studies on cortical tubule apical membranes revealed that mTOR inhibition markedly reduces ENaC activity, but does not alter activity of K^+ inwardly rectifying channels (ROMK channels). Together, these results demonstrate that mTOR regulates kidney tubule ion handling and suggest that mTOR regulates Na^+ homeostasis through SGK1-dependent modulation of ENaC activity.

mTORC2 regulates renal tubule sodium uptake by promoting ENaC activity

Catherine E. Gleason,[1] Gustavo Frindt,[2] Chih-Jen Cheng,[3] Michael Ng,[1] Atif Kidwai,[1] Priyanka Rashmi,[1] Florian Lang,[4] Michel Baum,[3] Lawrence G. Palmer,[2] and David Pearce[1]

[1]Department of Medicine, Division of Nephrology, UCSF, San Francisco, California, USA. [2]Department of Physiology and Biophysics, Weill Cornell Medical College, Cornell University, New York, New York, USA. [3]Department of Pediatrics and Medicine, University of Texas Southwestern, Dallas, Texas, USA. [4]Department of Physiology, University of Tübingen, Tübingen, Germany.

The epithelial Na^+ channel (ENaC) is essential for Na^+ homeostasis, and dysregulation of this channel underlies many forms of hypertension. Recent studies suggest that mTOR regulates phosphorylation and activation of serum/glucocorticoid regulated kinase 1 (SGK1), which is known to inhibit ENaC internalization and degradation; however, it is not clear whether mTOR contributes to the regulation of renal tubule ion transport. Here, we evaluated the effect of selective mTOR inhibitors on kidney tubule Na^+ and K^+ transport in WT and *Sgk1*$^{-/-}$ mice, as well as in isolated collecting tubules. We found that 2 structurally distinct competitive inhibitors (PP242 and AZD8055), both of which prevent all mTOR-dependent phosphorylation, including that of SGK1, caused substantial natriuresis, but not kaliuresis, in WT mice, which indicates that mTOR preferentially influences ENaC function. PP242 also substantially inhibited Na^+ currents in isolated perfused cortical collecting tubules. Accordingly, patch clamp studies on cortical tubule apical membranes revealed that mTOR inhibition markedly reduces ENaC activity, but does not alter activity of K^+ inwardly rectifying channels (ROMK channels). Together, these results demonstrate that mTOR regulates kidney tubule ion handling and suggest that mTOR regulates Na^+ homeostasis through SGK1-dependent modulation of ENaC activity.

Introduction

Sodium is the major cation in the extracellular fluid, and regulation of its reabsorption and excretion by the kidney plays a primary role in the homeostatic maintenance of fluid volume, body ion composition, and blood pressure (1). Although the majority of Na^+ reabsorption occurs in the proximal tubule, the distal nephron, particularly the aldosterone-sensitive distal nephron (ASDN), is responsible for fine-tuning of tubule fluid and for determining the net amount of Na^+ and K^+ excreted in the urine in response to changes in dietary intake (2). In cells of the ASDN, the rate-limiting and principal regulated step in Na^+ reabsorption is mediated by the apical membrane epithelial Na^+ channel (ENaC), which is controlled by several hormonal and nonhormonal regulators. The combined effect of these regulators is to activate signaling pathways that lead to increased ENaC abundance and activity (3). Importantly, inappropriate activation of ENaC is a primary mechanism in hypertension due to single gene defects (such as Liddle's syndrome) and has been implicated in essential (idiopathic) hypertension (4). In addition, factors influencing the production and action of aldosterone, the principal hormone involved in regulation of Na^+ and K^+ balance in the ASDN, have been implicated in more than 10% of hypertension (5, 6). Hypertension is the most prevalent cardiovascular disorder and is one of the leading causes of morbidity and mortality in the United States and worldwide (7). Multiple signals are integrated in the control of Na^+ balance, and a greater understanding of the implicated signaling pathways is essential for the rational design of novel hypertension therapeutics.

Serum/glucocorticoid regulated kinase 1 (SGK1) is a key signaling intermediate for activation of Na^+ reabsorption in the ASDN. Studies from many laboratories have demonstrated in vitro that SGK1 prevents ubiquitin-mediated proteasomal and/or lysosomal-dependent degradation of ENaC and promotes its accumulation at the apical plasma membrane (8). There is also evidence suggesting that SGK1 can additionally influence ENaC activity through direct physical interaction and phosphorylation of the C terminus of the αENaC subunit (9). Highlighting the importance of SGK1 in renal ENaC stimulation, mice with genetic ablation of *Sgk1* have significantly elevated aldosterone levels and exhibit Na^+ wasting and low blood pressure when fed a low-Na^+ diet (10), while on a high-K^+ diet, these mice develop hyperkalemia despite markedly elevated aldosterone. Interestingly, consistent with the idea that other regulatory mechanisms are also at play, direct measurements of ENaC activity indicate that the channels can be upregulated in the absence of SGK1 (11).

SGK1 is a member of the AGC family of serine/threonine protein kinases that includes, among others, AKT and PKC (12). In the ASDN, SGK1 is uniquely under dual regulation: its expression is rapidly induced by the mineralocorticoid aldosterone, and its catalytic activation is stimulated by phosphorylation (13, 14). Whereas mechanisms underlying aldosterone-stimulated regulation of *Sgk1* gene expression have been extensively studied and characterized, much less is understood about the molecular mechanisms involved in regulation of SGK1 catalytic activity. Like other AGC family members, SGK1 requires an initial "gateway" phosphory-

Conflict of interest: The authors have declared that no conflict of interest exists.
Submitted: October 24, 2013; **Accepted:** October 23, 2014.
Reference information: *J Clin Invest*. 2015;125(1):117–128. doi:10.1172/JCI73935.

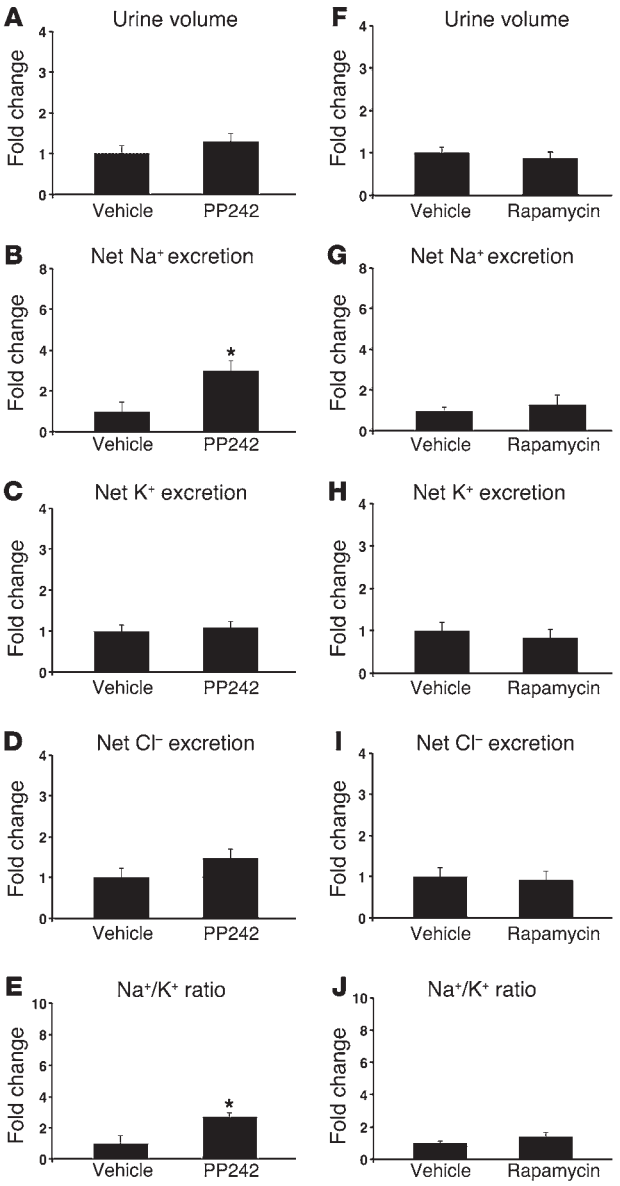

Figure 1. mTOR is required for Na^+ retention in vivo. WT mice were treated with (**A**–**E**) the catalytic site mTOR inhibitor PP242 (30 mg/kg i.p., n = 6 mice per treatment group) or (**F**–**J**) the mTORC1 inhibitor rapamycin (1.5 mg/kg i.p., n = 6 mice per treatment group), and urine was collected for 6 hours using balance cages (see Methods). Values for (**A** and **F**) urine volume, (**B** and **G**) net Na^+ excretion (calculated as urinary Na^+ × volume [mmol/6 h]), (**C** and **H**) net K^+ excretion (urinary K^+ × vol), (**D** and **I**) net Cl^- excretion (urinary Cl^- × vol), and (**E** and **J**) urinary Na^+/K^+ concentration ratio represent fold change relative to the vehicle-treated group. Data represent mean ± SEM; differences were determined by unpaired Student's t test. *$P < 0.05$ vs. vehicle.

lation at a site within its C-terminal hydrophobic motif (S422), followed by phosphorylation at a second site within the activation loop (T256) for complete catalytic activation. Phosphoinositide-dependent kinase 1 (PDK1) has been well established as the activation loop kinase, and more recently, mTOR was identified as the hydrophobic motif kinase (12, 15, 16).

mTOR exists in 2 evolutionarily conserved complexes, mTORC1 and mTORC2, and controls a diverse array of physiological processes, including protein translation, proliferation, migration, and metabolism. The downstream effectors targeted by mTOR and their subsequent physiological effects are determined by the protein complex within which mTOR resides. mTORC1 consists of mLST8, DEPTOR, PRAS40, and RAPTOR and is the complex responsible for mediating hormone- and growth factor–induced modulation of cell growth and proliferation. mTORC2 also contains mLST8 and DEPTOR, but is defined by the presence of RICTOR, mSIN1, and PROTOR. The presence of RAPTOR in mTORC1 confers sensitivity of this complex to the macrolide rapamycin. Conversely, mTORC2 is relatively insensitive to rapamycin due to the absence of RAPTOR (17). Only recently, with the generation of specific catalytic-site inhibitors of mTOR (termed TORKinibs), has it been possible to distinguish between mTORC1 and mTORC2 (18). Using the TORKinib PP242 in addition to genetic depletion of *Rictor* or *Raptor*, we previously demonstrated in cultured cells that mTORC2 is the hydrophobic motif kinase for SGK1 and that its activity is required for ENaC-dependent Na^+ reabsorption (15). PP242, unlike rapamycin, equally inhibits the kinase regardless of whether it is in mTORC2 or mTORC1. Together, the inhibitor and knockdown data strongly support the idea that in addition to cytoskeletal rearrangement and metabolism, mTORC2 also plays a key role in regulation of ion transport in cultured cells. However, a role for mTOR in regulation of Na^+ balance in vivo has not been addressed, nor has the role for SGK1 in mediating potential effects of mTOR. In vivo characterization of this signaling pathway is particularly important in this context because of the potential for compensation and counter-regulation of one nephron segment for another, which is not seen in cell culture experiments.

The aim of our present study was to determine whether whole-animal Na^+ balance is regulated by mTORC2, and if so, whether it exerts its effect by regulating ENaC in the ASDN. Capitalizing on the development of potent and highly selective chemical inhibitors, we used a pharmacological approach to acutely inactivate total mTOR catalytic activity in vivo in both WT and *Sgk1*$^{-/-}$ mice. We also examined mTOR-dependent activation of ENaC directly in intact tubules using in vitro microperfusion and patch clamp approaches. Our results suggested that mTORC2 is required for normal Na^+ reabsorption, acting primarily through regulation of ENaC.

Results

mTOR regulates Na^+ reabsorption in vivo. The recent development of TORKinibs, specific catalytic site inhibitors of mTOR, has allowed for characterization of distinct physiological functions for mTORC1 and mTORC2 (18). Previously, we used the TORKinib PP242 to demonstrate in the mouse cortical collecting duct (CCD) cell line mpkCCD that mTORC2-mediated SGK1 phosphorylation is required for generating ENaC-dependent Na^+ current (15). To determine whether mTOR activity is required in vivo for renal Na^+ retention, we treated WT mice with 30 mg/kg PP242 i.p. and collected their urine over the ensuing 6 hours (Figure 1, A–E). mTOR inhibition led to a significant increase in net Na^+ excretion and a trend toward increased urine output compared with vehicle-treated mice (Figure 1, A and B, and Table 1); the latter did not reach statistical significance, possibly due to the short half-life of PP242

Table 1. Urinary electrolytes in WT mice

	Vehicle (*n* = 6)	PP242 (*n* = 6)	Vehicle + amiloride (*n* = 6)	PP242 + amiloride (*n* = 6)	Vehicle + HCTZ (*n* = 9)	PP242 + HCTZ (*n* = 9)
Body mass (g)	22.6 ± 0.8	23± 0.3	22.5 ± 1.3	20.8 ± 2.0	22.0 ± 1.4	22.0 ± 1.3
Urine volume (μl/6 h)	196.3 ± 36.7	255.7 ± 39.5	288.7 ± 25.8	287.5 ± 60.5	223.8 ± 20.8	401.4 ± 33.3[A]
Na (mM)	22.2 ± 7.1	64.5 ± 10.5[A]	188.8 ± 29.2	187.2 ± 22.3	158.3 ± 12.4	137.8 ± 12.2
K (mM)	294.6 ± 42.5	235 ± 25.1	108.0 ± 9.8	90.0 ± 17.8	268 ± 24.5	193.1 ± 9.7[A]
Cl (mM)	147.2 ± 25.3	157 ± 21.7	172.7 ± 26.1	180.5 ± 31.3	278.1 ± 11.5	206.9 ± 8.2
Net Na^+ excretion (mmol/6 h)	5.26 ± 2.4	15.7 ± 2.6[A]	52.4 ± 6.2	48.0 ± 7.4	35.8 ± 4.2	55.1 ± 6.8[A]
Net K^+ excretion (mmol/6 h)	53.4 ± 8.6	57.9 ± 7.6	30.8 ± 3.6	20.9 ± 2.0[A]	59.9 ± 7.7	77.9 ± 7.6
Net Cl^- excretion (mmol/6 h)	26.5 ± 5.5	39.02 ± 6.2	48.0 ± 5.9	43.1 ± 4.8	61.7 ± 5.3	82.7 ± 7.1[A]
Urinary Na^+/K^+ concentration ratio	0.1 ± 0.05	0.27 ± 0.03[A]	1.7 ± 0.1	2.27 ± 0.2[A]	0.65 ± 0.1	0.73 ± 0.1
Creatinine (mg/dl)	55.9 ± 6.4	48.1 ± 7.4	38.6 ± 3.2	30.0 ± 4.1	46.1 ± 3.6	29.0 ± 1.4[A]
Glucose (mg/dl)	96.0 ± 12.3	301.4 ± 35.6[A]	56.2 ± 4.2	682.5 ± 233[A]	82.7 ± 5.5	895.3 ± 211[A]

Male WT mice (8–12 weeks old) were treated with vehicle or PP242, with or without amiloride or HCTZ (see Methods). After injection, mice were placed in balance cages for 6 hours under conditions of free access to food and water. Urine was collected, and urinary electrolytes, glucose, and creatinine were measured. Data represent mean ± SEM; differences were determined by unpaired Student's *t* test. [A]$P < 0.05$ vs. respective vehicle control.

(19). Furthermore, Na^+ concentration, but not K^+ or Cl^- concentration, was significantly increased in urine of PP242-treated mice, which in turn led to a significant increase in the urinary Na^+/K^+ concentration ratio (Figure 1, B–E), suggestive of an ENaC-dependent process. Rapamycin treatment, which inhibits only mTORC1, had no diuretic effect, and the urine concentration as well as the net excretion of Na^+ and K^+ were similar in vehicle- and rapamycin-treated mice (Figure 1, F–J, and Supplemental Table 1). These results suggest that mTOR-dependent Na^+ reabsorption is mediated by mTORC2 in vivo, as it is in cultured cells.

To confirm the efficacy of PP242 and rapamycin on in vivo inhibition of mTOR activity, we collected kidneys 1 hour after i.p. injection of vehicle control, PP242, or rapamycin. Kidney lysates were then processed for immunoblot analysis. Phosphospecific antibodies were used to detect phosphorylation of the mTOR substrates AKT and S6 ribosomal protein (RPS6). RPS6 is phosphorylated by p70S6K, a direct substrate of mTORC1. Because of the poor quality of the phosphospecific SGK1 hydrophobic motif antibody for detection of the endogenous phosphoprotein (15, 20), in order to measure SGK1 phosphorylation, we assessed the disappearance of slower-migrating forms of SGK1 using an antibody against total SGK1. The slower-migrating forms of SGK1 observed with SDS-PAGE (Figure 2A) represent mono- and hyperphosphorylated forms of SGK1 (21, 22). Kidney cytosolic extract was also prepared from an *Sgk1*$^{-/-}$ mouse for use as a control for detection of phosphorylated SGK1. Phosphorylation of the mTOR substrates AKT, SGK1, and RPS6 was significantly inhibited at 1 hour after injection of PP242 compared with vehicle control (Figure 2, A and B). Consistent with its primary effect on mTORC1 inhibi-

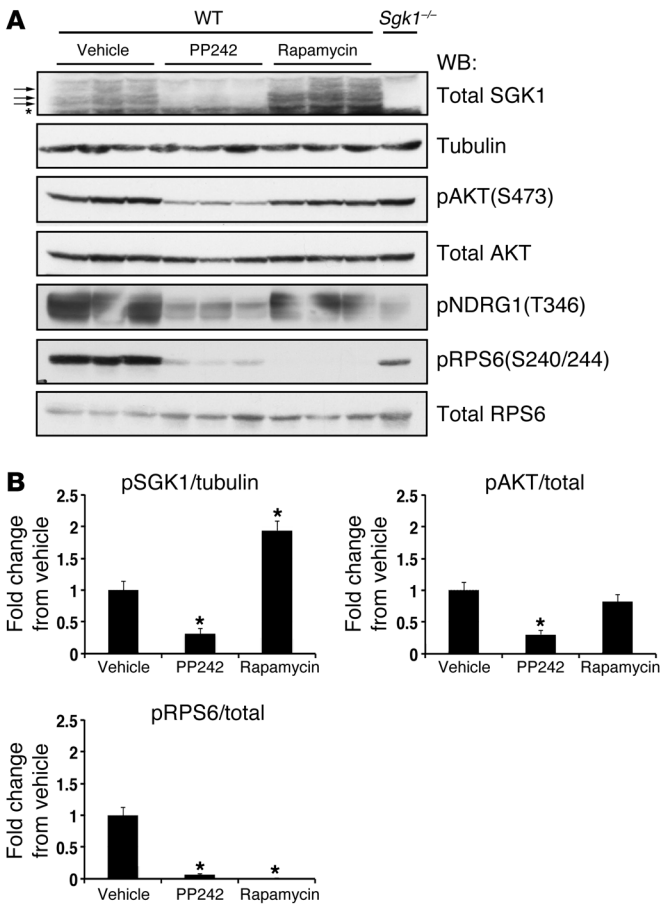

Figure 2. Efficacy of mTOR inhibition by PP242 or rapamycin in the kidney. WT mice were injected with vehicle, PP242, or rapamycin (*n* = 3 mice per treatment). At 1 hour after i.p. injection, kidneys were excised and snap frozen until preparation of cytosolic fractions. (**A**) Cytosolic extract (50–100 μg) was used to assess phosphorylation of SGK1, AKT, RPS6, and NDRG1 by Western blot (see Methods). *Sgk1*$^{-/-}$ kidney cytosolic lysate was used as a control to identify SGK1 phosphorylation. Each lane represents a separate mouse. (**B**) Quantification of Western blots, performed using NIH ImageJ. For SGK1, phosphorylation (**A**, arrows) was quantified by first correcting for the amount of the fastest-migrating SGK1 band in each lane (**A**, asterisk) and then correcting for the amount of tubulin in each lane. Phospho-AKT(S473) and phospho-RPS6(240/244) were corrected for total AKT and RPS6, respectively. Graphs represent fold change relative to the vehicle-treated group. Data represent mean ± SEM; differences were determined by unpaired Student's *t* test. *$P < 0.05$ vs. vehicle.

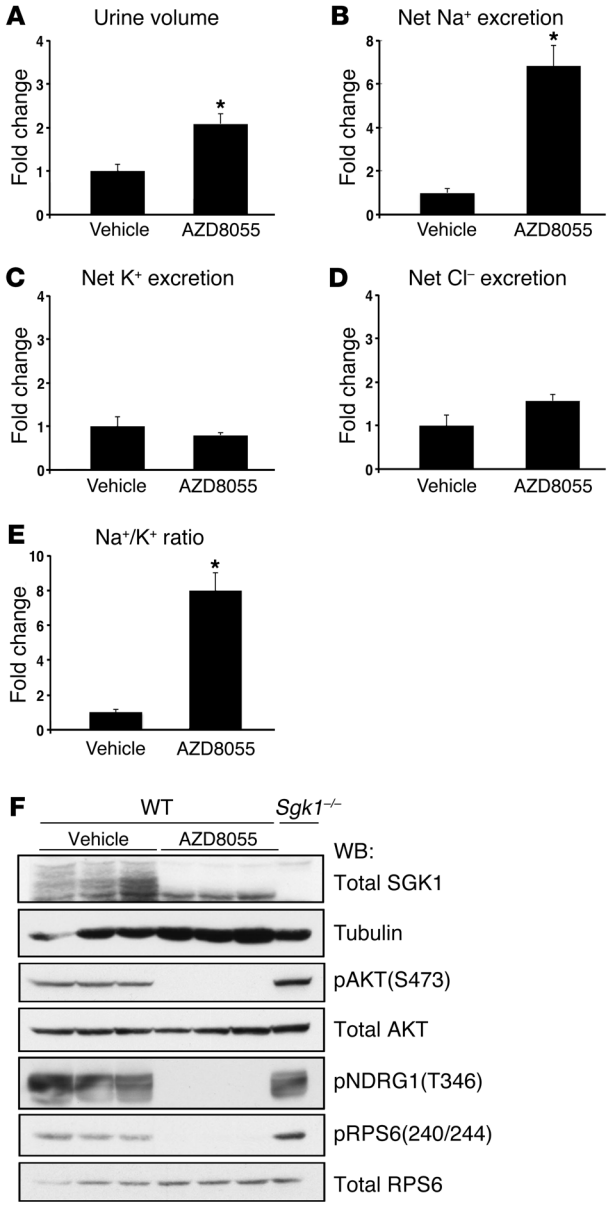

Figure 3. mTOR inhibition with the structurally distinct TORKinib AZD8055 blocks Na^+ reabsorption. WT mice were treated with AZD8055 (15 mg/kg i.p.), and urine was collected for 6 hours using balance cages as in Figure 1 (n = 6 mice per treatment group). Values for (**A**) urine volume, (**B**) net Na^+ excretion, (**C**) net K^+ excretion, (**D**) net Cl^- excretion, and (**E**) urinary Na^+/K^+ concentration ratio represent fold change relative to the vehicle-treated group. Data represent mean ± SEM; differences were determined by unpaired Student's t test. *$P < 0.05$ vs. vehicle. (**F**) Western blot of cytosolic fraction lysates prepared from kidneys treated for 1 hour with vehicle or AZD8055 (15 mg/kg i.p.) (n = 3 per treatment). Cytosolic fraction (50–100 μg) was used to detect phosphorylation of SGK1, AKT, NDRG1, and RPS6. SGK1 phosphorylation was assessed as in Figure 1. *Sgk1*$^{-/-}$ kidney cytosolic fraction was used a control for identification of SGK1 phosphorylation. Each lane represents a separate mouse.

tion, rapamycin treatment led to significant inhibition of RPS6 phosphorylation without blocking AKT or SGK1 phosphorylation. In addition, phosphorylation of the SGK1 and AKT target N-MYC–downregulated gene 1 (NDRG1) (23) was inhibited by PP242, but not by rapamycin (Figure 2A).

To control for possible off-target effects of PP242, we treated WT mice with a newly available, structurally distinct ATP-competitive small-molecule mTOR inhibitor, AZD8055 (24). Like PP242, AZD8055 is highly selective for mTOR, only inhibiting other PI3K family members (class I and III PI3Ks) when used at >1,000-fold higher doses than those required to inhibit mTOR (19, 24). AZD8055 also has a longer half-life than PP242, which we speculated could be more effective in balance studies. Compared with vehicle control, AZD8055 completely abolished RPS6 and AKT(S473) phosphorylation and blocked the appearance of slower-migrating (hyperphosphorylated) forms of SGK1 in kidney cytosolic lysates from WT mice treated for 1 hour (Figure 3F). As expected, phosphorylation of the NDRG1 was also completely blocked by AZD8055 (Figure 3F). To examine the effect of AZD8055 on Na^+ and K^+ balance, WT mice were injected i.p. with 15 mg/kg AZD8055 and then placed in balance cages for collection of urine over a 6-hour period, as in Figure 1. AZD8055 led to a significant diuresis that was 2-fold greater than vehicle control (Figure 3, A, and Supplemental Table 2). Consistent with the significant increase in urine output, AZD8055-treated mice had a striking 7-fold increase in net Na^+ excretion (Figure 3B and Supplemental Table 2). In contrast to the effect on Na^+ reabsorption, urine K^+ concentration was significantly decreased in mice receiving AZD8055, and net K^+ and Cl^- excretion were the same as those of vehicle-treated controls (Figure 3, C and D, and Supplemental Table 2). mTOR inhibition with AZD8055 also led to a significant increase in the urine Na^+/K^+ concentration ratio (Figure 3E). The finding that AZD8055 treatment caused urine electrolyte excretion similar to that of PP242 supports the specificity of these compounds to inhibit mTOR and further suggests that mTOR modulates Na^+ balance predominantly through regulation of ENaC. It seems likely that the more striking diuretic and natriuretic effects of AZD8055 primarily reflect its longer half-life and, to a lesser extent, its greater potency.

Inhibition of ENaC with amiloride blocks the natriuretic effect of PP242. The "potassium-sparing" natriuresis induced by PP242 treatment suggests a specific effect of mTORC2 on ENaC. However, since mTOR is known to have pleiotropic effects, it is possible that mTOR controls Na^+ reabsorption by modulating the activity or membrane abundance of additional ion transporters or exchangers. Accordingly, SGK1, a major target of mTORC2, has been shown in vitro to have effects on various transporters and exchangers, most notably the NaCl cotransporter (NCC) in the distal collecting tubule (DCT) (25). To begin to address whether mTORC2 acts predominantly on ENaC, we examined the effects of mTOR inhibition on Na^+ excretion in mice treated with either amiloride to inhibit ENaC or with hydrochlorothiazide (HCTZ) to block NCC activity. In the presence of amiloride, the effect of mTOR inhibition was lost: urine output, urine Na^+ concentration, and net Na^+ excretion were not significantly different from vehicle control (Figure 4, A–D, and Table 1). In contrast, in the presence of HCTZ, mTOR inhibition still led to a significant increase in urine output and net Na^+ excretion above that observed with HCTZ treatment alone (Figure 4, E–H, and Table 1). Interestingly, K^+ secretion was significantly reduced in mice receiving both amiloride and PP242, but not with the combination of

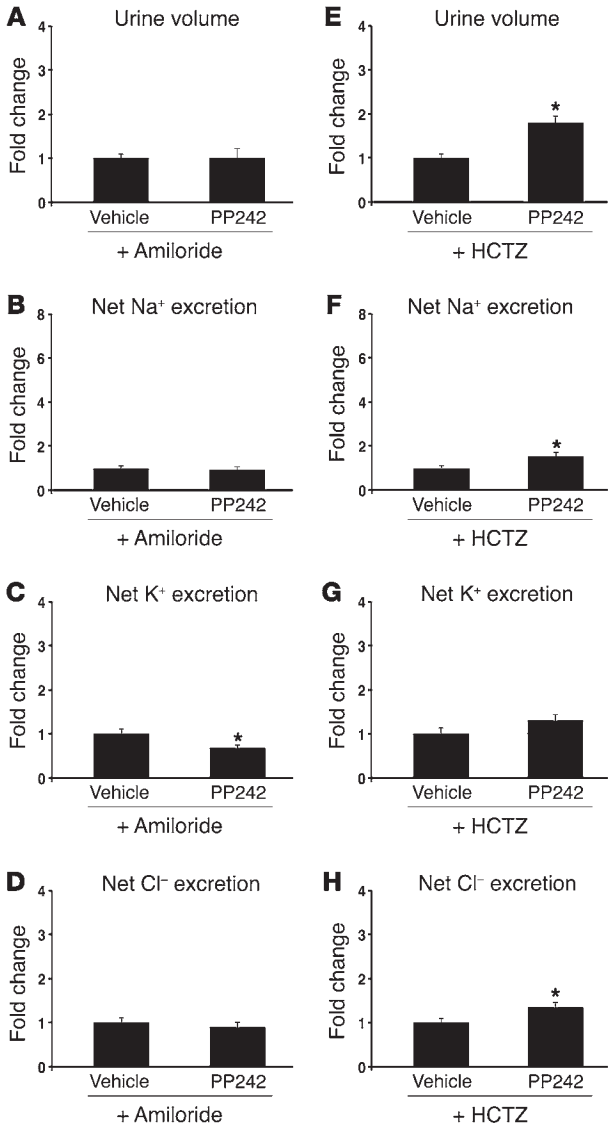

Figure 4. Inhibition of ENaC with amiloride blunts the natriuretic effect of PP242. WT mice were (**A**–**D**) pretreated overnight with amiloride to block ENaC, then injected i.p. the next morning with amiloride plus vehicle or PP242 (n = 6 mice per treatment group), or (**E**–**H**) pretreated overnight with HCTZ to block NCC, then injected i.p. the next morning with HCTZ plus vehicle or PP242 (n = 9 mice per treatment group); subsequently, urine was collected for 6 hours using balance cages (see Methods). Values for (**A** and **E**) urine volume, (**B** and **F**) net Na^+ excretion, (**C** and **G**) net K^+ excretion, (**D** and **H**) and net Cl^- excretion represent fold change relative to the vehicle-treated group. Data represent mean ± SEM; differences were determined by unpaired Student's t test. *$P < 0.05$ vs. vehicle.

HCTZ and PP242 (Figure 4, C and G). Together, these results suggest that ENaC activity is required for PP242-induced natriuresis and provide further evidence that ENaC is a primary target of mTORC2 in regulation of Na^+ balance. As the natriuretic effect of PP242 appeared to be blunted in the presence of HCTZ compared with PP242 alone, it is possible that mTOR functions in a minor capacity to regulate NCC function. Interestingly, this role of mTOR was accentuated in *Sgk1*$^{-/-}$ mice (see below).

mTORC2 is required for ENaC-dependent transepithelial potential difference in perfused CCDs in vitro. The above results suggest that mTOR activity within mTORC2 — but not mTORC1 — is required for ENaC-dependent Na^+ transport in vivo, hence explaining the natriuretic effect exerted by PP242 and AZD8055. To directly examine the effect of mTOR on ENaC-dependent Na^+ transport, we examined transepithelial potential difference (PD) generated in isolated intact CCDs treated with PP242 or rapamycin (Figure 5). CCDs harvested from WT mice were pretreated with the mineralocorticoid deoxycorticosterone acetate (DOCA), then subjected to in vitro microperfusion as previously described (26). After establishing a baseline PD (–9.1 ± 2.8 mV), PP242 was added to the bathing solution, which resulted in a significant decrease in the lumen negative PD to –4.9 ± 1.3 mV. Removal of PP242 (washout) resulted in an increase in the lumen negative PD to –7.0 ± 1.7 mV, which was not significantly different from baseline. Addition of amiloride to the lumen caused the potential to reach a value not different from 0 (Figure 5A), which confirmed that the PD generated was due to ENaC. Importantly, consistent with the in vivo results, inhibition of mTORC1 alone with rapamycin had no effect on the transepithelial PD (Figure 5B). These results provide direct support for the concept that mTOR inhibition disrupts ENaC-dependent transepithelial Na^+ transport and suggest that this effect is specifically caused by inhibition of mTORC2.

mTORC2 is required for apical membrane ENaC-mediated Na^+ current: direct measurement by patch clamp. To assess directly the effect of mTOR inhibition on apical membrane ENaC-mediated Na^+ current, we performed whole-cell patch-clamp experiments on microdissected CCDs. After Sprague-Dawley rats were pretreated with low-Na^+ diet to stimulate ENaC, tubules were isolated, split open, and preincubated for 30 minutes in solutions containing either 1 μM PP242 or diluent (see Methods). Consistent with our in vivo and microperfusion findings, PP242 inhibition of mTOR dramatically inhibited ENaC function, measured as amiloride-sensitive whole-cell Na^+ current (Figure 6A). In contrast to its suppression of ENaC, PP242 had no effect on patch clamp recordings of K^+ flux via K^+ inwardly rectifying channels (ROMK channels), measured as tertiapin-Q–sensitive (TPNQ-sensitive) whole-cell current (Figure 6B).

αENaC abundance and cleavage are unchanged after PP242 inhibition of mTOR. A common mechanism for regulation of ion transport involves posttranslational modifications, including phosphorylation, ubiquitinylation, and enzymatic cleavage, that together determine both the abundance and the activity of transporters at the plasma membrane. The E3 ubiquitin ligase NEDD4-2 has been shown in vitro to target both NCC and ENaC for proteasomal or lysosomal degradation. Degradation of NCC or ENaC can by blocked by phosphorylation of NEDD4-2 at S322 and S328 by SGK1, which creates binding sites for 14-3-3 proteins and disrupts interaction with ENaC or NCC (25, 27). To begin to establish a mechanism for PP242-induced natriuresis, we first examined phosphorylation of NEDD4-2 in kidney cytosolic extracts 1 hour after i.p. injection of vehicle, PP242, or AZD8055. mTOR inhibition with PP242 significantly decreased NEDD4-2 phosphorylation at S328 (Figure 7A), which suggests that mTOR might be involved in regulating NEDD4-2 phosphorylation. AZD8055 treatment also tended to reduce NEDD4-2 phosphorylation; however, this decrease did not reach statistical significance (Figure 7B), likely

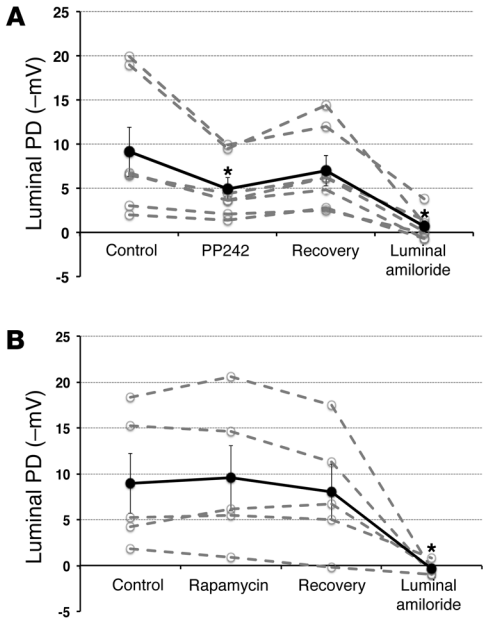

Figure 5. mTORC2 is the mTOR complex responsible for stimulation of Na^+ uptake in the CCD and is required for ENaC-dependent transepithelial Na^+ transport: in vitro microperfusion. Microdissected mouse kidney CCDs were perfused in vitro. After a baseline PD was established (control), PP242 (**A**; $n = 7$ individual experiments) or rapamycin (**B**; $n = 5$ individual experiments) was added to the bath solution, and PD was measured once a steady state was achieved. PD recovery was measured after washout of PP242 or rapamycin. Amiloride was added at the end of the experiment to measure the contribution of ENaC to the generation of the PD. Solid black line denotes average of individual experiments (dashed gray lines). Data represent mean ± SEM; differences were determined by repeated-measures 1-way ANOVA. $^*P < 0.05$ vs. control.

due to variability of staining with the anti–phospho–NEDD4-2 antibody. Interestingly, both PP242 and AZD8055 induced a decrease in NEDD4-2 protein, which suggests that mTOR might also participate in stabilization of NEDD4-2.

Next, we examined whether mTOR inhibition decreases the abundance of ENaC or NCC protein. To allow time for mTOR inhibition to influence membrane accumulation of ENaC or NCC or cleavage of ENaC, we prepared total membrane fractions from kidneys collected 3 hours after injection of vehicle, PP242, or AZD8055. Surprisingly, there was no significant difference in membrane levels of full-length or cleaved αENaC among treatment groups (Figure 8, A and B). Similarly, there was no significant difference in membrane levels of NCC phosphorylation or total protein in mice treated with AZD8055; however, PP242 treatment led to a significant increase in NCC phosphorylation and abundance (Figure 8, A and C). The basis of this finding is unclear; however, it is notable that PP242 has a short half-life, and we found its inhibitory effect on phosphorylation of SGK1 and AKT was abated by 3 hours after treatment (Supplemental Figure 1). Thus, mTOR activity appears to be required for NEDD4-2 phosphorylation and possibly NCC phosphorylation and abundance, implying a novel role for mTOR in these processes. However, our data do not support regulation of ENaC protein abundance or proteolytic cleavage as a primary mechanism for regulation of Na^+ reabsorption through mTOR.

Figure 6. mTORC2 is required for ENaC-mediated Na^+ current: direct measurement by patch clamp. The effect of mTOR on ENaC and ROMK activity was assessed by whole-cell patch clamp of microdissected rat kidney CCD. After isolation, tubules were preincubated for 30 minutes with or without 1 μM PP242. (**A**) Currents through ENaC (I_{Na}) were measured as the difference in current at V_m –100 mV with and without 10^{-5} M amiloride. $n = 17$ (PP242) and 24 (control) cells from 4 animals. (**B**) Currents through ROMK (I_{SK}) were measured as the difference in current at V_m –100 mV with and without 10^{-7} M TPNQ. $n = 20$ (PP242) and 23 (control) cells from 4 animals. Data represent mean ± SEM; differences were determined by repeated-measures 1-way ANOVA. $^*P < 0.05$ vs. vehicle.

mTOR inhibition unveils complex compensatory mechanisms for ion homeostasis in Sgk1$^{-/-}$ mice. Previous in vitro work from our lab demonstrated that phosphorylation of SGK1 by mTORC2 is required for optimal Na^+ flux through ENaC. *Sgk1*$^{-/-}$ mice have pseudohypoaldosteronism with high aldosterone levels, Na^+ wasting on a low-Na^+ diet (10, 11, 28), and hyperkalemia on a high-K^+ diet (29). Compared with mice with functional mutations in ENaC subunits or mice with disruption of mineralocorticoid receptor expression, which exhibit lethality due to extreme Na^+ wasting (30), the *Sgk1*$^{-/-}$ phenotype is very mild. This has led to speculation that kinases other than SGK1 can mediate ENaC activation in response to aldosterone, or that renin-angiotensin-aldosterone system–mediated (RAAS-mediated) hyperactivation of other ion transporters (such as NHE3 or NCC) provides sufficient compensatory Na^+ reabsorption. In addition to SGK1, mTORC2 is the hydrophobic motif kinase for several other AGC family serine/threonine protein kinases, including AKT. In vitro data have suggested a role for AKT in regulation of ENaC-mediated Na^+ reuptake (31, 32), although this concept is controversial. In order to determine whether SGK1 is the primary mTORC2 target involved in mediating the effect of mTORC2 on ENaC, we treated *Sgk1*$^{-/-}$ mice with vehicle or PP242 and measured urine volume and electrolytes. Similar to WT mice, PP242 treatment led to a significant increase in net Na^+ excretion in *Sgk1*$^{-/-}$ mice; however, in marked contrast to the WT mice, PP242 induced a significant increase in net excretion of K^+ and Cl^- in *Sgk1*$^{-/-}$ mice (Figure 9, A–D, and Table 2).

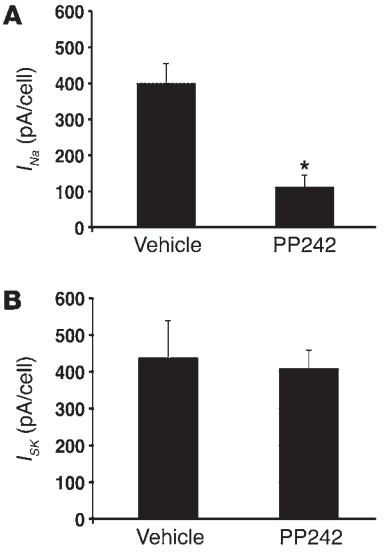

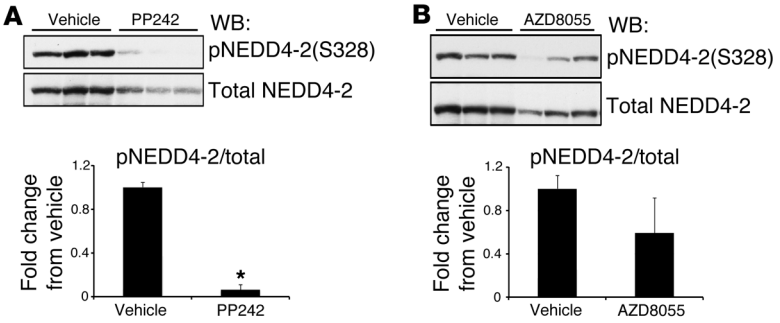

Figure 7. NEDD4-2 phosphorylation and protein abundance are regulated by mTOR. WT mice were injected i.p. with (**A**) PP242 or (**B**) AZD8055 or vehicle control (n = 3 mice per treatment). At 1 hour after injection, kidneys were excised and snap frozen until preparation of cytosolic fractions. Cytosolic extract (100 μg) was used to assess phosphorylation of NEDD4-2(S328) or total NEDD4-2 by Western blot (see Methods). Each lane represents a separate mouse. Quantification of Western blots is also shown (performed using NIH ImageJ); phosphorylation of NEDD4-2 was corrected for the amount of total NEDD4-2 protein, and values represent fold change relative to the vehicle-treated group. Data represent mean ± SEM; differences were determined by unpaired Student's t test. *$P < 0.05$ vs. vehicle.

Furthermore, the PP242-mediated increase in the urinary Na^+/K^+ concentration ratio (Figure 9E) was significantly lower in *Sgk1*$^{-/-}$ than WT mice (1.6-fold vs. 2.7-fold; $P < 0.01$, unpaired Student's t test). Thus, in contrast to WT mice, the urine electrolyte excretion pattern observed in PP242-treated *Sgk1*$^{-/-}$ mice did not reflect selective inhibition of ENaC. Rather, it appeared that chronic deletion of *Sgk1* activates compensatory Na^+ reabsorption pathways that are independent of SGK1, but sensitive to mTOR inhibition.

In order to assess the relative contributions of ENaC and NCC to mTOR-dependent Na^+ transport in *Sgk1*$^{-/-}$ mice, we treated *Sgk1*$^{-/-}$ mice with a combination of PP242 and either HCTZ or amiloride (Figure 10 and Supplemental Table 3), as performed earlier with WT mice (Figure 4). Similar to WT mice, amiloride treatment prevented the PP242-induced natriuresis and completely blocked the PP242-induced kaliuresis and chloruresis in *Sgk1*$^{-/-}$ mice (Figure 10, A–D). In marked contrast to WT mice, when ENaC activity was blocked by amiloride, *Sgk1*$^{-/-}$ mice became lethargic as well as markedly hyperkalemic, with K^+ values exceeding 10 mM (data not shown). In fact, the combination of PP242 and amiloride in some cases was lethal. Inhibition of NCC by HCTZ in *Sgk1*$^{-/-}$ mice was also similar to that in WT mice, as PP242 elicited a small but significant natriuresis above that induced by HCTZ treatment alone. Similar to ENaC inhibition, HCTZ also prevented PP242-induced K^+ and Cl^- secretion. Importantly, the combination of HCTZ and PP242 did not stimulate significant urine output or significant excretion of Cl^- (Figure 10, E–H), as was observed in WT mice. Thus, in *Sgk1*$^{-/-}$ mice, as in WT mice, mTOR inhibition stimulated natriuresis partly through regulation of ENaC activity. However, in *Sgk1*$^{-/-}$ mice, we also observed mTOR-dependent compensatory upregulation of NCC activity, identifying mTOR as a novel regulator of NCC.

Discussion

The maintenance of ion homeostasis by the renal tubules requires an array of hormonal and non-hormonal signals to be integrated by intracellular signaling networks that control activity of ion transporters in multiple nephron segments. In the distal nephron, where fine tuning of Na^+ and K^+ balance occurs, a large body of in vivo and in vitro evidence supports a central role for SGK1 as a signal integrator. SGK1 regulates the net activity of multiple transporters, most notably that of ENaC (33). Recent data from cell culture models supports the idea that mTOR, and specifically mTORC2, is a key upstream component of this signaling network, which controls SGK1 activity through phosphorylation of a serine near its C terminus within a short domain termed the hydrophobic motif (15, 20, 34). However, in vivo evidence for mTORC2-dependent control of Na^+ transport is lacking. In vivo characterization of these signaling networks is particularly important because of the potential for compensation and interaction between nephron segments.

Notably, a recent study reported kidney-specific inactivation of mTORC1 and mTORC2, alone and in combination. Genetic inactivation of mTORC1, or mTORC1 and mTORC2 together, caused gross developmental tubule defects (35). Here, we used 2 chemically distinct mTOR catalytic site inhibitors, PP242 and AZD8055, to determine whether mTOR functions in vivo to acutely regulate tubule Na^+ and K^+ handling, and if so, whether it involves regulation of SGK1 phosphorylation and subsequent ENaC activation in the distal nephron. The use of chemically unrelated inhibitors minimizes the chance that off-target effects are responsible for our findings and allows for assessment of acute effects on ion transport without the potential for confounding effects due to altered tubule development or adaptation to prolonged mTOR inactivation.

By treating mice with either PP242 or AZD8055, or with the mTORC1-specific inhibitor rapamycin, we demonstrated that mTORC2, but not mTORC1, participates in the regulation of Na^+ reabsorption. Importantly, we found that mTOR inhibition with either TORKinib enhanced Na^+ excretion, but not K^+ excretion, consistent with a primary effect on ENaC (1). Moreover, the effect of mTOR inhibition was lost when ENaC activity was blocked by amiloride, but not when NCC activity was blocked by HCTZ. These data provide further evidence that in WT mice on a normal-salt diet, mTOR influences Na^+ transport predominantly through ENaC, as opposed to NCC. Finally, when ENaC activity was directly assessed by microperfusion and patch clamp, we found that its activity was mTOR dependent. Together, these data strongly support the concept that mTORC2 — but not mTORC1 — acts in vivo as a key upstream regulator of ENaC. In light of the importance of rapamycin as a therapeutic agent, these observations have important clinical implications in addition to shedding new light on the mechanistic basis of ion transport regulation.

Despite prior in vitro evidence that SGK1 regulates various tubule transporters in addition to ENaC, notably NHE3, NCC, SGLT1, and ROMK (28, 33), our present data do not support a major role for these transporters in mediating the physiological effects of mTORC2 on Na^+ reabsorption in WT mice. Combined natriuresis and kaliuresis would be expected if activation of NHE3, SGLT1, NKCC2, or NCC were impaired by mTOR inhibition, and this was

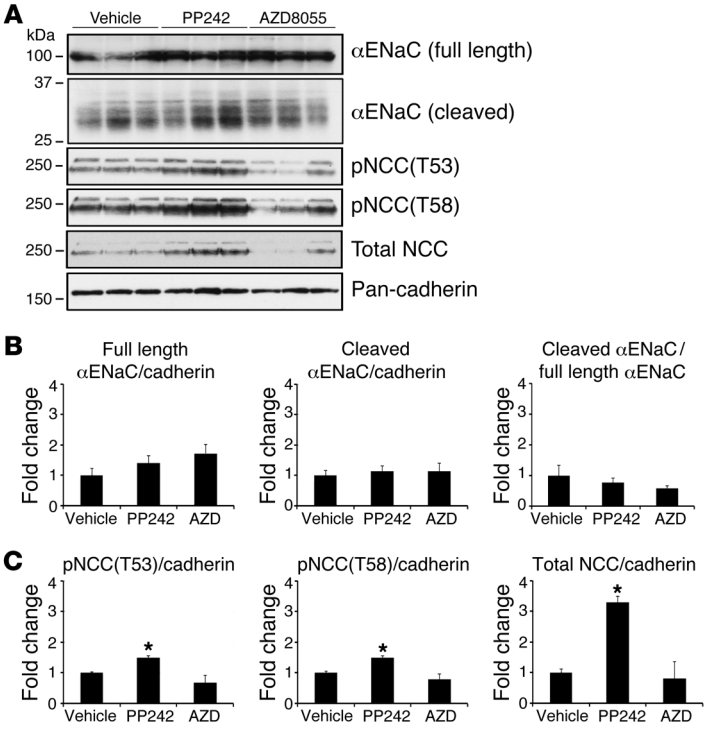

Figure 8. mTOR inhibition does not diminish αENaC abundance or cleavage, nor NCC phosphorylation or abundance. WT mice were injected with vehicle, PP242, or AZD8055 (n = 3 mice per treatment). At 3 hours after i.p. injection, kidneys were excised and snap frozen until preparation of total membrane fractions (see Methods). (**A**) Total membrane fractions (100 μg) were used to assess full-length and cleaved αENaC by Western blot using an antibody that recognizes the N terminus of αENaC. Phosphorylation of NCC and total NCC were assessed using antibodies against phospho-NCC(T53), phospho-NCC(T58), and total NCC. Each lane represents a separate mouse. (**B**) Quantification of full-length and cleaved αENaC Western blots, either corrected by cadherin level in each lane or expressed as cleaved/full-length αENaC ratio; values represent fold change relative to the vehicle-treated group. (**C**) Quantification of phosphorylated and total NCC Western blots (performed using NIH ImageJ), corrected for the level of cadherin in each lane; values represent fold change relative to the vehicle-treated group. Data represent mean ± SEM; differences were determined by unpaired Student's t test. *$P < 0.05$ vs. vehicle.

not observed. Furthermore, blocking NCC activity with HCTZ did not prevent significant diuresis and natriuresis from occurring upon mTOR inhibition. Although the urine excretion data could be attributed in part to ROMK inhibition, our patch clamp data did not support this: PP242 inhibited ENaC-dependent Na^+ current, but had no effect on ROMK, consistent with a previous in vitro report demonstrating that SGK1 is selective for ENaC and does not stimulate ROMK (36). Interestingly, combined treatment with PP242 and amiloride led to a significant decrease in net K^+ excretion compared with amiloride treatment alone (Figure 4C). Although the mechanisms underlying this observation are currently unclear, we speculate that mTOR could have an independent effect on K^+ flux through activation of K^+ channels — possibly BK channels — that is uncovered in the presence of ENaC inhibition. Consistent with this idea, amiloride-insensitive K^+ secretion has been observed in rodents (37). Finally, mTORC2 has been implicated in mediating the effects of insulin on glucose metabolism (38), and mice treated with PP242 developed hyperglycemia and glycosuria (Table 1 and C.E. Gleason, unpublished observations). Hence, osmotic diuresis could have contributed to the observed natriuresis, yet it is unlikely to be a major factor, since it would cause combined kaliuresis and natriuresis. Furthermore, in the presence of amiloride, although PP242 induced glycosuria, electrolyte excretion was the same in vehicle- and PP242-treated mice (Figure 4 and Table 1).

The relative importance of increases in ENaC open probability (P_o) versus the number of channels present in the plasma membrane (N) in mediating hormonal stimulation of tubule Na^+ reabsorption is still a matter of debate. Studies support both modes of regulation (39, 40), and it seems likely that both are involved. SGK1 has been found to have effects on both P_o and N, at least in part through inhibition of the E3 ubiquitin ligase NEDD4-2 (27, 41), and possibly through effects on the phosphorylation state (9) and proteolytic processing (11, 28) of the channel itself. It is notable in this regard that NEDD4-2, although primarily associated with effects on N, has also been associated with effects on P_o (42). In the present study, we found that mTOR inhibition blunted NEDD4-2 phosphorylation and protein abundance. Although PP242 and AZD8055 decreased NEDD4-2 phosphorylation and blocked ENaC-dependent Na^+ reabsorption, neither TORKinib altered the expression of full-length or processed αENaC in plasma membrane fractions. There was, however, a trend for AZD8055 to inhibit NCC phosphorylation and overall expression. This effect did not reach statistical significance, and further studies are needed to determine whether mTOR has a direct role in regulating NEDD4-2 and NCC phosphorylation or protein stability. It is interesting to note that in *Sgk1*$^{-/-}$ mice, phosphorylation of NEDD4-2 and phosphorylation and total protein levels of NCC are markedly reduced (11, 28, 43). In contrast, little effect has been observed on ENaC overall abundance or apical membrane expression, despite marked reduction in amiloride-sensitive transepithelial PD (10). Our present data support the idea that in vivo, mTOR regulates ENaC activity primarily by influencing P_o, rather than by trafficking, subunit cleavage, or protein stability. However, this issue remains unresolved, with data supporting both possibilities (11, 39). Since the abundance of ENaC at the plasma membrane is likely to vary between tubule segments, we may have missed a difference in ENaC membrane abundance or cleavage in our whole-kidney membrane preparations.

Unless placed under extraordinary Na^+ restriction or K^+ excess, *Sgk1*$^{-/-}$ mice ultimately come into Na^+ and K^+ balance (albeit with decreased blood pressure and glomerular filtration rate, and markedly elevated blood levels of aldosterone). Importantly, the RAAS adapts to perturbations within hours to days, and hence *Sgk1*$^{-/-}$ mice

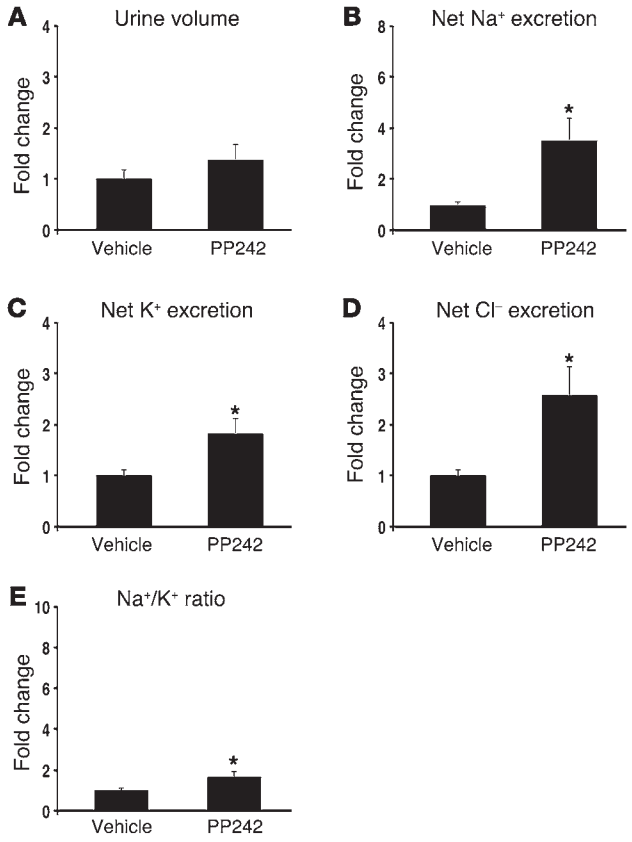

Figure 9. mTOR inhibition in *Sgk1*$^{-/-}$ mice uncovers activation of alternative compensatory Na$^+$ reabsorption pathway(s). *Sgk1*$^{-/-}$ mice were treated i.p. with PP242 (30 mg/kg) or vehicle (n = 9 mice per treatment group), and urine was collected for 6 hours using balance cages as in Figure 1. Values for (**A**) urine volume, (**B**) net Na$^+$ excretion, (**C**) net K$^+$ excretion, (**D**) net Cl$^-$ excretion, and (**E**) urinary Na$^+$/K$^+$ concentration ratio are expressed as fold change relative to the vehicle-treated group. Data represent mean ± SEM; differences were determined by unpaired Student's t test. *P < 0.05 vs. vehicle.

— even if inducible (with gene deletion taking take days to weeks to achieve) — suffer from the confounding effects of adaptation (28). In contrast, mineralocorticoid receptor–KO mice die within 2 weeks of birth from Na$^+$ wasting and hyperkalemia, and thus have a more severe phenotype (30). It has been postulated that marked elevation of aldosterone allows *Sgk1*$^{-/-}$ mice to compensate for diminished ENaC activity by upregulation of other ion transporters or non-SGK1-dependent activation of ENaC. Thus, whether ENaC is selectively regulated by SGK1, or whether other signaling molecules can also regulate ENaC in a physiologically relevant manner, becomes a question of considerable importance. There have been conflicting reports based on cell culture and oocyte studies regarding the roles of several SGK1 relatives (31, 32, 44–46). Furthermore, there have been conflicting reports regarding the effects of SGK1 on transporters other than ENaC. In this regard, it is interesting that in *Sgk1*$^{-/-}$ mice, we uncovered an mTOR-dependent Na$^+$ reabsorptive pathway, which does not have the urinary electrolyte pattern of purely ENaC-dependent Na$^+$ reabsorption. Rather, under conditions of compensation to SGK1 deficiency, it appears that mTOR inhibition blocks not only ENaC, but also one or more of the upstream transporters.

Our present study as well as other work found that *Sgk1*$^{-/-}$ mice were particularly sensitive to ENaC inhibition: amiloride treatment induced severe hyperkalemia and death (C.E. Gleason, unpublished observations, and ref. 47). The sensitivity of *Sgk1*$^{-/-}$ mice to ENaC inhibition suggests that an important component of the compensatory mechanism involves an SGK1-independent increase in ENaC activity. Interestingly, we found that amiloride also prevented the natriuresis induced by mTOR inhibition, supporting the idea that mTOR regulates ENaC activity even in the absence of SGK1. As mentioned above, *Sgk1*$^{-/-}$ mice exhibited greatly elevated aldosterone levels, and it is well known that aldosterone influences ENaC function not only through stimulation of SGK1, but also through induction of αENaC transcription, and possibly other mediators (11). We hypothesize that the elevated RAAS activity in *Sgk1*$^{-/-}$ mice stimulates compensatory ENaC activity through SGK1-independent, mTOR-dependent mechanisms.

It is also interesting that the role of NCC in *Sgk1*$^{-/-}$ mice appeared to be different than that in WT mice: NCC blockade with thiazide in *Sgk1*$^{-/-}$ mice prevented the PP242-induced kaliuresis and chloruresis, which suggests that *Sgk1*$^{-/-}$ mice also exhibit mTOR-dependent compensatory upregulation of NCC. Based on these observations, we hypothesize that in *Sgk1*$^{-/-}$ mice, NCC is upregulated above baseline, while ENaC activity is brought back toward baseline by the marked elevation in RAAS activity. Thus, mTOR appears to be implicated in the control of both NCC and ENaC, as its inhibition caused a mixed electrolyte excretion profile. Further studies will be needed to determine which signaling molecules, and which transporters, mediate mTOR-dependent effects under conditions of compensation to *Sgk1* gene deletion and chronic ion transport perturbation by diuretics. However, taken together, our results support the concept that in WT animals, mTORC2-dependent Na$^+$ reabsorption occurs predominantly through SGK1-dependent regulation of ENaC.

Table 2. Urinary electrolytes in *Sgk1*$^{-/-}$ mice

	Vehicle (n = 9)	PP242 (n = 9)
Body mass (g)	27.3 ± 0.2	29.5 ± 2.8
Urine volume (μl/6 h)	292.0 ± 48.8	402.8 ± 84.8
Na (mM)	36.1 ± 4.5	85.8 ± 18.2^A
K (mM)	174.7 ± 15.8	236.4 ± 21.1^A
Cl (mM)	100.7 ± 13.8	170.9 ± 24.2^A
Net Na$^+$ excretion (mmol/6 h)	9.4 ± 0.9	33.1 ± 7.9^A
Net K$^+$ excretion (mmol/6 h)	48.1 ± 5.8	88.1 ± 14.7^A
Net Cl$^-$ excretion (mmol/6 h)	26.1 ± 3.2	67.1 ± 15.0^A
Urinary Na$^+$/K$^+$ concentration ratio	0.21 ± 0.03	0.35 ± 0.05^A
Creatinine (mg/dl)	47.7 ± 4.2	44.4 ± 4.1
Glucose (mg/dl)	61.9 ± 5.7	94.9 ± 12.8^A

Male *Sgk1*$^{-/-}$ mice (8–12 weeks old) were treated with vehicle or PP242 (see Methods). After injection, mice were placed in balance cages for 6 hours under conditions of free access to food and water. Urine was collected, and urinary electrolytes, glucose, and creatinine were measured. Data represent mean ± SEM; differences were determined by unpaired Student's t test. ^{A}P < 0.05 vs. vehicle.

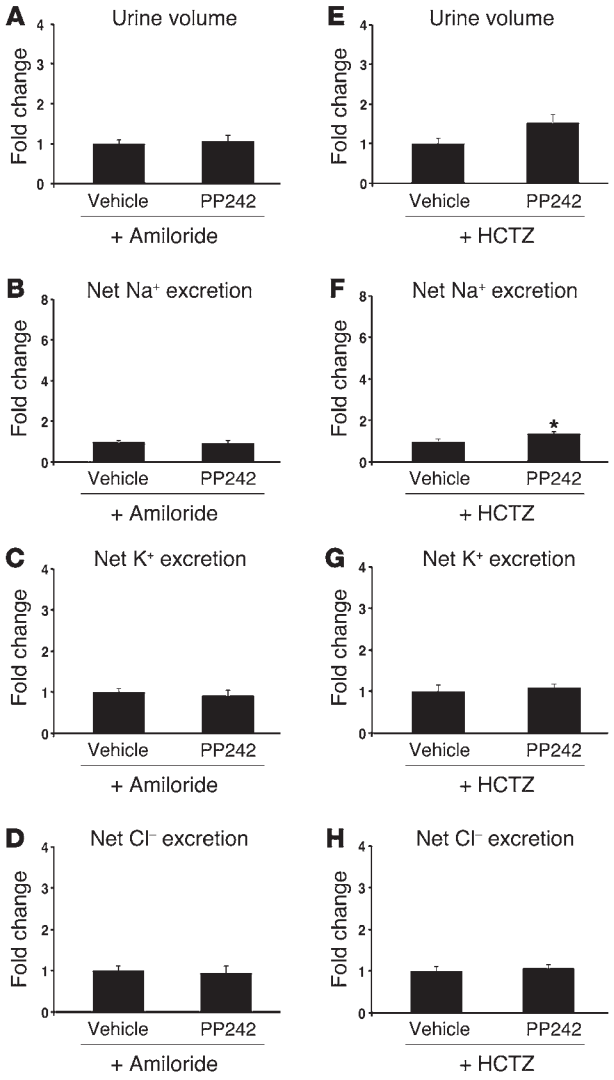

Figure 10. In *Sgk1*$^{-/-}$ mice, mTOR regulates both ENaC and NCC. *Sgk1*$^{-/-}$ mice were (**A**–**D**) pretreated overnight with amiloride to block ENaC, then injected i.p. the next morning with amiloride plus vehicle (n = 7 mice) or PP242 (n = 8 mice), or (**E**–**H**) pretreated overnight with HCTZ to block NCC, then injected i.p. the next morning with HCTZ plus vehicle or PP242 (n = 7 mice per treatment group); subsequently, urine was collected for 6 hours using balance cages (see Methods). Values for (**A** and **E**) urine volume, (**B** and **F**) net Na^+ excretion, (**C** and **G**) net K^+ excretion, (**D** and **H**) and net Cl^- excretion represent fold change relative to the vehicle-treated group. Data represent mean ± SEM; differences were determined by unpaired Student's t test. *$P < 0.05$ vs. vehicle.

Methods

Animals and genotype analysis. WT C57BL/6 mice used for PP242, AZD8055, and rapamycin in vivo studies were purchased from Jackson Laboratory. The derivation of the *Sgk1*$^{-/-}$ line has been reported previously (10). *Sgk1*$^{+/-}$ mice were bred inter se to obtain *Sgk1*$^{-/-}$ mice. Genotyping was performed by PCR analysis of genomic DNA isolated from tail snips of newborn mice (10).

Na^+ and K^+ balance studies. WT C57BL/6 or *Sgk1*$^{-/-}$ mice (8–12 weeks old) were kept in balance cages for an acclimatization period of 3 days with free access to water and food (Picolab standard diet 20, 0.3% Na; catalog no. 5053, LabDiets). After 3 days of acclimatization, vehicle or PP242 solution was injected i.p. at a final dose of 30 mg/kg body weight. PP242 solution was prepared by dissolving powdered PP242 (gift from K. Shokat, UCSF, San Francisco, California, USA) in a sterile saline solution containing 20% DMSO and 40% polyethelene glycol (PEG); vehicle solution contained saline with 20% DMSO and 40% PEG without PP242. Urine was collected 6 hours after injection and stored at 4°C. Urine samples were sent to Stanford University Department of Comparative Medicine Diagnostic Laboratory for determination of urine parameters. Similar experiments were performed with rapamycin or AZD8055; 1.5 mg/kg rapamycin (Sigma-Aldrich) and 15 mg/kg AZD8055 (SelleckChem) were prepared using the same vehicle as described for the PP242 solution.

For diuretic experiments, mice were placed in balance cages for an acclimatization period of 3 days with free access to food and water. In the afternoon of day 3 of acclimatization, for studies with amiloride, mice were given 20 mg/l amiloride (Sigma-Aldrich) in their drinking water. The following morning, mice were injected i.p. with either 5 mg/kg amiloride in vehicle or 5 mg/kg amiloride plus 30 mg/kg PP242; the vehicle used was the same as described above. For HCTZ experiments, in the afternoon of day 3 of acclimatization, mice were injected i.p. with 25 mg/kg HCTZ (Sigma-Aldrich) in the same vehicle used for all animal studies. The next morning, mice were injected i.p. with either 25 mg/kg HCTZ in vehicle or 25 mg/kg HCTZ plus 30 mg/kg PP242. In both diuretic studies, urine was collected for 6 hours after i.p. injection, and samples were sent to Stanford University Department of Comparative Medicine Diagnostic Laboratory for analysis of urine parameters.

Preparation of kidney cytosolic and total membrane extracts. C57BL/6 mice were placed on a low-Na^+ diet (0.0–0.02% Na; TD 90228, Harlan Laboratories) for 5 days. On day 5 of the low-Na^+ diet, mice were injected i.p. with vehicle, 30 mg/kg PP242, 15 mg/kg AZD8055, or 1.5 mg/kg rapamycin. Kidneys were excised 1 or 3 hours after injection and snap-frozen in liquid nitrogen. Frozen kidneys were homogenized by crushing with a mortar and pestle on dry ice. The powdered kidney was collected into eppendorf tubes and lysed using buffers contained in the Plasma Membrane Fractionation kit (Biovision), and cytosolic and total membrane protein fractions were prepared according to the manufacturer's protocol. 50–100 μg cytosolic fraction or total membrane fraction protein was run on SDS-PAGE and transferred to nitrocellulose for immunoblotting. Antibodies against phospho- and total AKT (catalog nos. 4060S and 9272S, respectively), phospho- and total RPS6 (catalog nos. 2215S and 2317S, respectively), and phospho-NDRG1 (catalog no. 5482S) were from Cell Signaling Technologies. SGK1 phosphorylation was assessed by examination of the phosphorylation-induced delay in mobility shift of the total protein (21, 22). Other antibodies were as follows: anti-SGK1 (catalog no. S5188, Sigma-Aldrich); anti–β-tubulin (catalog no. CP06, Calbiochem); anti–N-terminal αENaC (gift from J. Loffing, University of Zurich, Zurich, Switzerland); anti–phospho-NCC(T53), anti–phospho-NCC(T58), and anti-NCC (gifts from R. Fenton, Aarhus University, Denmark, Sweden); anti–phospho–NEDD4-2 (catalog no. ab95399, Abcam); anti–NEDD4-2 (catalog no. ab46521, Abcam).

In vitro microperfusion of CCDs. WT 129/sv mice (8–10 weeks old) were raised in a 12-hour day/12-hour night cycle and fed a normal salt diet (Harlan Teklad) and tap water ad libitum for 3–6 days before experiments. Because the transepithelial PD in the mouse

CCD is near 0, mice were administered deoxycorticosterone acetate (100 mg/kg body weight) for 5–7 days. Mice were then killed by CO_2 asphyxiation, and their kidneys were removed quickly, sliced in thin coronal sections, and placed in Hanks' solution containing 137 mM NaCl, 5 mM KCl, 0.8 mM $MgSO_4$, 0.33 mM Na_2HPO_4, 0.44 mM KH_2PO_4, 1 mM $MgCl_2$, 10 mM tris (hydroxymethyl) amino methane hydrochloride, 0.25 mM $CaCl_2$, 2 mM glutamine, and 2 mM L-lactate at 4°C. CCD segments were then dissected freehand and transferred to a 1-ml temperature-controlled bathing chamber. Tubules were perfused in vitro as previously described (26). Briefly, isolated CCDs were perfused with an ultrafiltrate-like solution containing 115 mM NaCl, 25 mM $NaHCO_3$, 2.3 mM Na_2HPO_4, 10 mM Na acetate, 1.8 mM $CaCl_2$, 1 mM $MgSO_4$, 5 mM KCl, 8.3 mM glucose, and 5 mM alanine. The bathing solution had the same composition except that it contained 6 g/dl albumin. Transepithelial PD was measured with a Keithley 6517A programmable electrometer using the perfusion pipette as the bridge into the tubular lumen. The reference electrode was in the bathing solution. After a steady-state PD was measured, either 0.1 μM rapamycin or 1 μM PP242 was added to the bathing solution. Once a steady state was achieved, the drug was removed, and the PD was measured again. Amiloride (10^{-8} M; Sigma-Aldrich) was added to the bathing solution at the end of the experiment to inhibit ENaC.

Patch clamp. Sprague-Dawley rats of either gender (150–200 g; Charles River Laboratories) raised free of viral infections were used for all experiments. Animals were fed a synthetic low-Na^+ diet containing <0.005% NaCl (Harlan Teklad) for 1 week. Measurement of whole-cell Na^+ currents in principal cells of the CCD followed previously described procedures (48, 49). Split-open tubules were superfused with solutions prewarmed to 37°C containing 135 mM Na methanesulfonate, 5 mM KCl, 2 mM Ca methanesulfonate, 1 mM $MgCl_2$, 2 mM glucose, 5 mM Ba methanesulfonate, and 10 mM HEPES, adjusted to pH 7.4 with NaOH. Patch-clamp pipettes were filled with solutions containing 7 mM KCl, 123 mM aspartic acid, 20 mM CsOH, 20 mM TEAOH, 5 mM EGTA, 10 mM HEPES, 3 mM MgATP, and 0.3 mM NaGDPβS, with pH adjusted to 7.4 with KOH. The total concentration of K^+ was ~120 mM. Net Na^+ fluxes through Na^+ channels were measured as the difference in current with and without 10^{-5} M amiloride (Sigma-Aldrich) in the bath. For measurements of whole-cell K^+ currents, Ba^{2+} was omitted from the superfusate. The pipette solutions contained 7 mM KCl, 123 mM aspartic acid, 5 mM EGTA, and 10 mM HEPES, with pH adjusted to 7.4 with KOH. The total concentration of K^+ was approximately 140 mM. Net K^+ fluxes through ROMK channels were measured as the difference in current with and without 10^{-7} M TPMQ (Sigma-Aldrich) in the bath (49). Pipettes were pulled from hematocrit tubing, coated with Sylgard, and fire polished with a microforge. Pipette resistances ranged 3–6 MΩ. Currents were measured with a List EPC-7 amplifier (Heka Elektronik). Voltages were controlled and currents recorded using a Digidata 1440A interface and PClamp 9 software (Axon Instruments).

Statistics. For balance studies with WT or *Sgk1*$^{-/-}$ mice and quantification of Western blots, statistical comparisons between vehicle- and drug-treated groups were analyzed by unpaired, 2-tailed Student's *t* test. For microperfusion and patch clamp experiments, statistical comparisons between groups were analyzed using repeated-measures 1-way ANOVA. For all comparisons, a *P* value less than 0.05 was considered statistically significant. Statistical analyses were performed using GraphPad Prism (version 5.0; GraphPad Software). All results are expressed as mean ± SEM.

Study approval. All experimental procedures involving animals were carried out in accordance with relevant laws and institutional guidelines approved by the IACUCs of the institutions at which animal experiments were performed (UCSF, University of Texas Southwestern, and Weill Cornell Medical College).

Acknowledgments

This research was supported by NIH grants from the National Institutes of Diabetes and Digestive and Kidney Diseases (DK56695 to D. Pearce; T32 DK007219 and K01 DK098313-02 to C.E. Gleason; DK41612 and DK078596 to M. Baum) and the O'Brien Center (P30DK 079328 to Peter Igarashi, PI – Physiology Core, M. Baum, co-PI; DK59659 to G. Frindt and L.G. Palmer) as well as by the James Hilton Manning and Emma Austin Manning Foundation (to D. Pearce). PP242 was a gift of Kevan Shokat and Morrie Feldman.

Address correspondence to: David Pearce, Mission Bay, Genentech Hall, Room N272C, 600 16th Street, San Francisco, California 94158, USA. Phone: 415.476.7015; E-mail: dpearce@medsfgh.ucsf.edu.

Chih-Jen Cheng's present address is: Division of Nephrology, Tri-Service General Hospital, Taipei, Taiwan.

Atif Kidwai's present address is: Department of Medicine, Tufts University School of Medicine, Salem, Massachusetts, USA.

1. Bubien JK. Epithelial Na+ channel (ENaC), hormones, and hypertension. *J Biol Chem*. 2010;285(31):23527–23531.
2. Loffing J, Korbmacher C. Regulated sodium transport in the renal connecting tubule (CNT) via the epithelial sodium channel (ENaC). *Pflugers Arch*. 2009;458(1):111–135.
3. Kashlan OB, Kleyman TR. Epithelial Na(+) channel regulation by cytoplasmic and extracellular factors. *Exp Cell Res*. 2012;318(9):1011–1019.
4. Suviolahti E, et al. Significant reduction of ATP production in PHA-activated $CD4^+$ cells in 1-day-old blood from transplant patients. *Transplantation*. 2012;94(12):1243–1249.
5. Sartorato P, et al. Inactivating mutations of the mineralocorticoid receptor in Type I pseudohypoaldosteronism. *Mol Cell Endocrinol*. 2004;217(1):119–125.
6. Rossier BC, Schild L. Epithelial sodium channel: mendelian versus essential hypertension. *Hypertension*. 2008;52(4):595–600.
7. Mittal BV, Singh AK. Hypertension in the developing world: challenges and opportunities. *Am J Kidney Dis*. 2010;55(3):590–598.
8. Pao AC. SGK regulation of renal sodium transport. *Curr Opin Nephrol Hypertens*. 2012;21(5):534–540.
9. Diakov A, Korbmacher C. A novel pathway of epithelial sodium channel activation involves a serum- and glucocorticoid-inducible kinase consensus motif in the C terminus of the channel's alpha-subunit. *J Biol Chem*. 2004;279(37):38134–38142.
10. Wulff P, et al. Impaired renal Na(+) retention in the sgk1-knockout mouse. *J Clin Invest*. 2002;110(9):1263–1268.
11. Fejes-Toth G, Frindt G, Naray-Fejes-Toth A, Palmer LG. Epithelial Na+ channel activation and processing in mice lacking SGK1. *Am J Physiol Renal Physiol*. 2008;294(6):F1298–F1305.
12. Arencibia JM, Pastor-Flores D, Bauer AF, Schulze JO, Biondi RM. AGC protein kinases: From structural mechanism of regulation to allosteric drug development for the treatment of human diseases. *Biochim Biophys Acta*. 2013;1834(7):1302–1321.
13. Lang F, Bohmer C, Palmada M, Seebohm G, Strutz-Seebohm N, Vallon V. (Patho)physiological significance of the serum- and glucocorticoid-inducible kinase isoforms. *Physiol Rev*.

2006;86(4):1151–1178.
14. McCormick JA, Bhalla V, Pao AC, Pearce D. SGK1: a rapid aldosterone-induced regulator of renal sodium reabsorption. *Physiology (Bethesda)*. 2005;20:134–139.
15. Lu M, et al. mTOR complex-2 activates ENaC by phosphorylating SGK1. *J Am Soc Nephrol*. 2010;21(5):811–818.
16. Pearce LR, Komander D, Alessi DR. The nuts and bolts of AGC protein kinases. *Nat Rev Mol Cell Biol*. 2010;11(1):9–22.
17. Laplante M, Sabatini DM. mTOR signaling at a glance. *J Cell Sci*. 2009;122(pt 20):3589–3594.
18. Feldman ME, Shokat KM. New inhibitors of the PI3K-Akt-mTOR pathway: insights into mTOR signaling from a new generation of Tor kinase domain inhibitors (TORKinibs). *Curr Top Microbiol Immunol*. 2010;347:241–262.
19. Feldman ME, et al. Active-site inhibitors of mTOR target rapamycin-resistant outputs of mTORC1 and mTORC2. *PLoS Biol*. 2009;7(2):e38.
20. Garcia-Martinez JM, Alessi DR. mTOR complex 2 (mTORC2) controls hydrophobic motif phosphorylation and activation of serum- and glucocorticoid-induced protein kinase 1 (SGK1). *Biochem J*. 2008;416(3):375–385.
21. Park J, Leong ML, Buse P, Maiyar AC, Firestone GL, Hemmings BA. Serum and glucocorticoid-inducible kinase (SGK) is a target of the PI 3- kinase-stimulated signaling pathway. *EMBO J*. 1999;18(11):3024–3033.
22. Wang J, et al. SGK integrates insulin and mineralocorticoid regulation of epithelial sodium transport. *Am J Physiol Renal Physiol*. 2001;280(2):F303–F313.
23. Sommer EM, Dry H, Cross D, Guichard S, Davies BR, Alessi DR. Elevated SGK1 predicts resistance of breast cancer cells to Akt inhibitors. *Biochem J*. 2013;452(3):499–508.
24. Chresta CM, et al. AZD8055 is a potent, selective, and orally bioavailable ATP-competitive mammalian target of rapamycin kinase inhibitor with in vitro and in vivo antitumor activity. *Cancer Res*. 2010;70(1):288–298.
25. Arroyo JP, et al. Nedd4-2 modulates renal Na^+-Cl^- cotransporter via the aldosterone-SGK1-Nedd4-2 pathway. *J Am Soc Nephrol*. 2011;22(9):1707–1719.
26. Sartorato P, Cluzeaud F, Fagart J, Viengchareun S, Lombes M, Zennaro MC. New naturally occurring missense mutations of the human mineralocorticoid receptor disclose important residues involved in dynamic interactions with deoxyribonucleic acid, intracellular trafficking, and ligand binding. *Mol Endocrinol*. 2004;18(9):2151–2165.
27. Debonneville C, et al. Phosphorylation of Nedd4-2 by Sgk1 regulates epithelial Na(+) channel cell surface expression. *EMBO J*. 2001;20(24):7052–7059.
28. Faresse N, et al. Inducible kidney-specific Sgk1 knockout mice show a salt-losing phenotype. *Am J Physiol Renal Physiol*. 2012;302(8):F977–F985.
29. Huang DY, et al. Impaired regulation of renal K+ elimination in the sgk1-knockout mouse. *J Am Soc Nephrol*. 2004;15(4):885–891.
30. Berger S, et al. Mineralocorticoid receptor knockout mice: pathophysiology of Na+ metabolism. *Proc Natl Acad Sci U S A*. 1998;95(16):9424–9429.
31. Arteaga MF, Canessa CM. Functional specificity of Sgk1 and Akt1 on ENaC activity. *Am J Physiol Renal Physiol*. 2005;289(1):F90–F96.
32. Lee IH, Dinudom A, Sanchez-Perez A, Kumar S, Cook DI. Akt mediates the effect of insulin on epithelial sodium channels by inhibiting Nedd4-2. *J Biol Chem*. 2007;282(41):29866–29873.
33. Lang F, Shumilina E. Regulation of ion channels by the serum- and glucocorticoid-inducible kinase SGK1. *FASEB J*. 2013;27(1):3–12.
34. Lu M, Wang J, Ives HE, Pearce D. mSIN1 protein mediates SGK1 protein interaction with mTORC2 protein complex and is required for selective activation of the epithelial sodium channel. *J Biol Chem*. 2011;286(35):30647–30654.
35. Grahammer F, et al. mTORC1 maintains renal tubular homeostasis and is essential in response to ischemic stress. *Proc Natl Acad Sci U S A*. 2014;111(27):E2817–E2826.
36. Chen S-Y, et al. Epithelial sodium channel regulated by aldosterone-induced protein sgk. *Proc Natl Acad Sci U S A*. 1999;96(5):2514–2519.
37. Frindt G, Palmer LG. K^+ secretion in the rat kidney: Na^+ channel-dependent and -independent mechanisms. *Am J Physiol Renal Physiol*. 2009;297(2):F389–F396.
38. Hagiwara A, et al. Hepatic mTORC2 activates glycolysis and lipogenesis through Akt, glucokinase, and SREBP1c. *Cell Metab*. 2012;15(5):725–738.
39. Loffing J, et al. Aldosterone induces rapid apical translocation of ENaC in early portion of renal collecting system: possible role of SGK. *Am J Physiol Renal Physiol*. 2001;280(4):F675–F682.
40. Staruschenko A. Regulation of transport in the connecting tubule and cortical collecting duct. *Compr Physiol*. 2012;2(2):1541–1584.
41. Bhalla V, et al. Serum- and glucocorticoid-regulated kinase 1 regulates ubiquitin ligase neural precursor cell-expressed, developmentally down-regulated protein 4-2 by inducing interaction with 14-3-3. *Mol Endocrinol*. 2005;19(12):3073–3084.
42. Wiemuth D, Ke Y, Rohlfs M, McDonald FJ. Epithelial sodium channel (ENaC) is multi-ubiquitinated at the cell surface. *Biochem J*. 2007;405(1):147–155.
43. Vallon V, Schroth J, Lang F, Kuhl D, Uchida S. Expression and phosphorylation of the Na^+-Cl^- cotransporter NCC in vivo is regulated by dietary salt, potassium, and SGK1. *Am J Physiol Renal Physiol*. 2009;297(3):F704–F712.
44. Pao AC, et al. Expression and role of serum and glucocorticoid-regulated kinase 2 in the regulation of Na^+/H^+ exchanger 3 in the mammalian kidney. *Am J Physiol Renal Physiol*. 2010;299(6):F1496–F1506.
45. Pao AC, et al. NH2 terminus of serum and glucocorticoid-regulated kinase 1 binds to phosphoinositides and is essential for isoform-specific physiological functions. *Am J Physiol Renal Physiol*. 2007;292(6):F1741–F1750.
46. Friedrich B, et al. The serine/threonine kinases SGK2 and SGK3 are potent stimulators of the epithelial Na^+ channel alpha,beta,gamma-ENaC. *Pflugers Arch*. 2003;445(6):693–696.
47. Artunc F, et al. Responses to diuretic treatment in gene-targeted mice lacking serum- and glucocorticoid-inducible kinase 1. *Kidney Blood Press Res*. 2009;32(2):119–127.
48. Frindt G, Palmer LG. Na channels in the rat connecting tubule. *Am J Physiol Renal Physiol*. 2004;286(4):F669–F674.
49. Frindt G, Shah A, Edvinsson J, Palmer LG. Dietary K regulates ROMK channels in connecting tubule and cortical collecting duct of rat kidney. *Am J Physiol Renal Physiol*. 2009;296(2):F347–F354.